Supplementary Information

Sequential Element Control of Non-Precious Dual Atom Catalysts on Mesoporous Carbon Nanotubes for High Performance Lithium-Oxygen Batteries

*Yeji Lim[a, †], Hongjun Chang[b, †], Huiju Kim[a], Yoon Jeong Yoo[a], YeoJin Rho[a], Bo Ran Kim[a], Hye Ryung Byon[c], Janghyuk Moon[b, *], Won-Hee Ryu[a, *]*

[a]Department of Chemical and Biological Engineering, Sookmyung Women's University, 100 Cheongpa-ro 47-gil, Yongsan-gu, Seoul, 04310, Republic of Korea

[b]Department of Energy Systems Engineering, Chung-Ang University, Heukseok-Ro, Dongjak-Gu, Seoul 06974, Republic of Korea

[c]Department of Chemistry, Korea Advanced Institute of Science and Technology (KAIST), Daejeon 34141, Republic of Korea

* Corresponding author

E-mail: whryu@sookmyung.ac.kr (Prof. Won-Hee Ryu), jhmoon84@cau.ac.kr (Prof. Janghyuk Moon)

† These authors contributed equally to this awork.

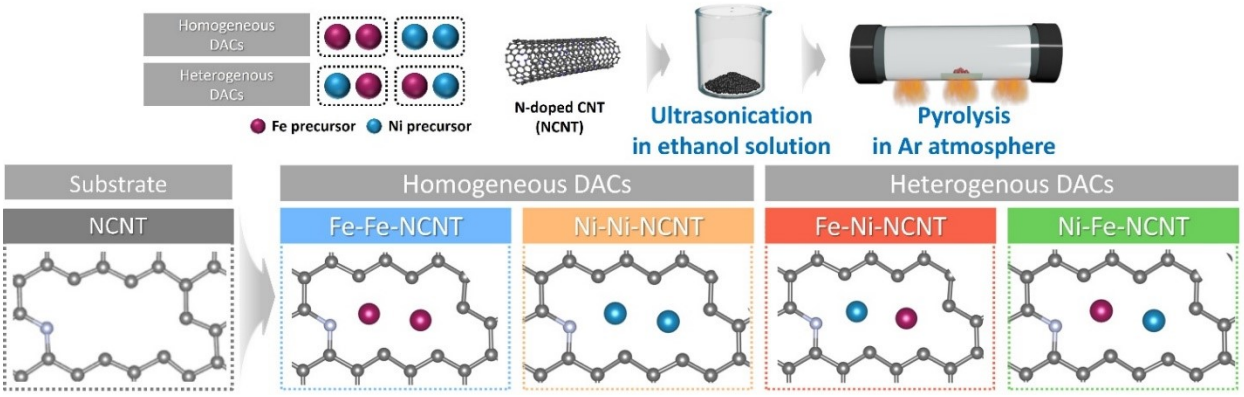

Figure S1. Schematic illustration of the synthesize method of homogeneous and heterogeneous DACs.

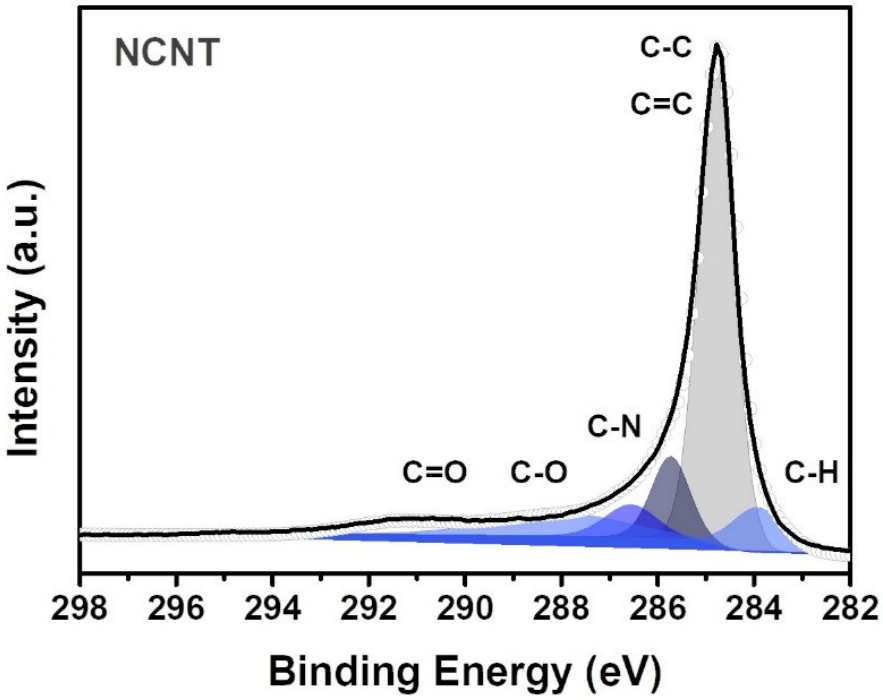

Figure S2. The X-ray photoelectron spectroscopy (XPS) spectra of C 1s obtained from the NCNT.

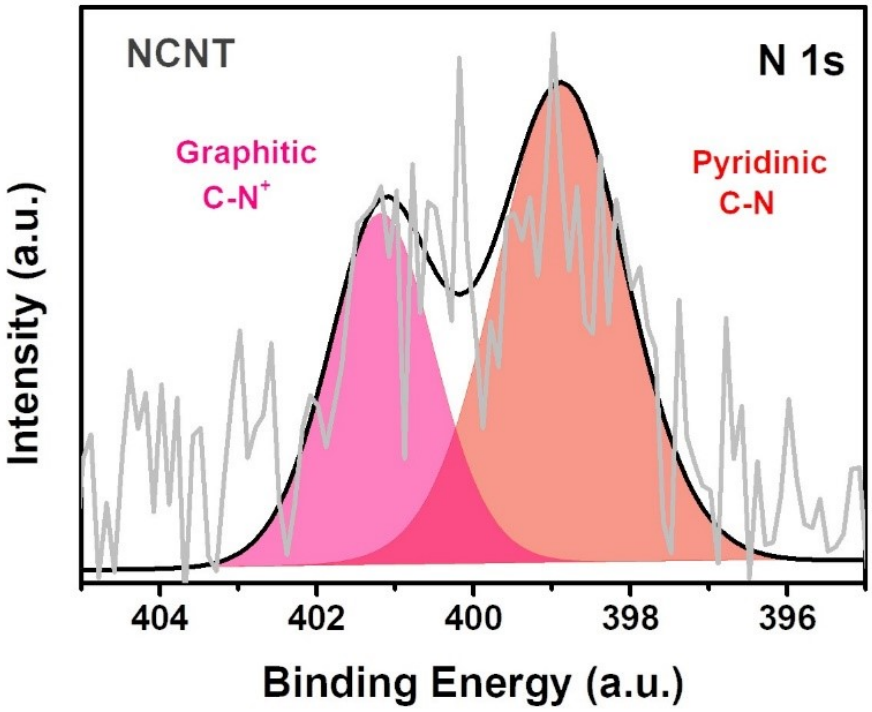

Figure S3. The X-ray photoelectron spectroscopy (XPS) spectra of N 1s obtained from the NCNT.

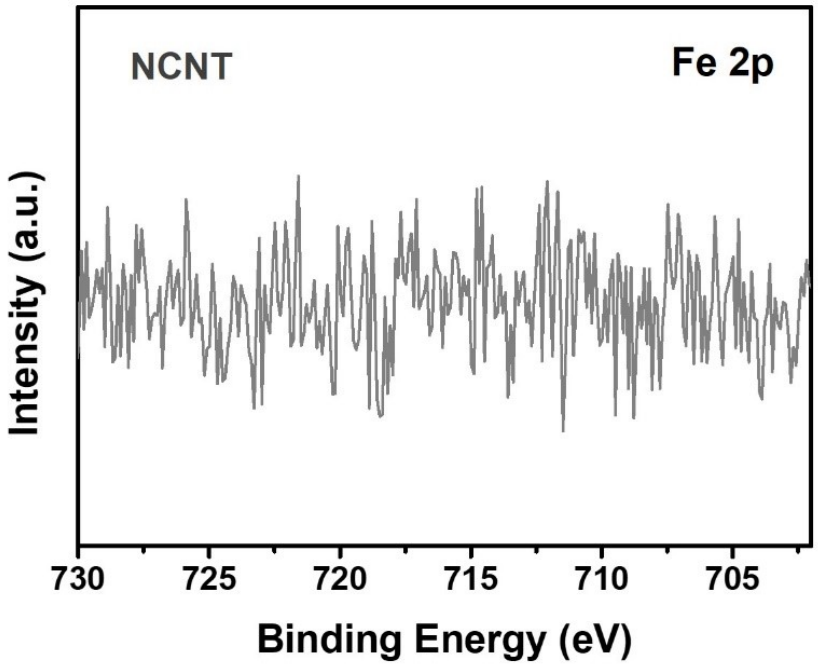

Figure S4. The X-ray photoelectron spectroscopy (XPS) spectra of Fe 2p obtained from the NCNT.

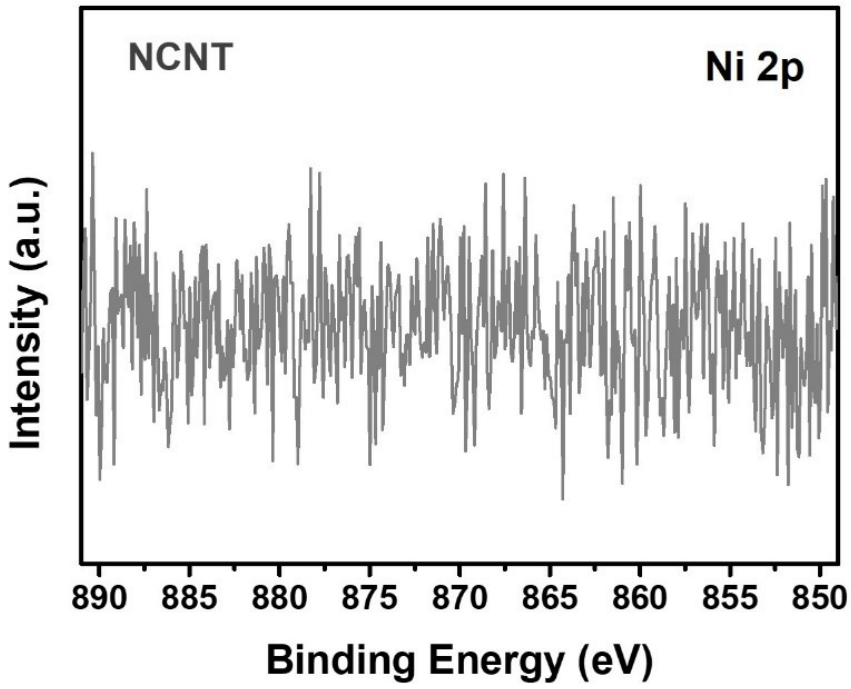

Figure S5. The X-ray photoelectron spectroscopy (XPS) spectra of Ni 2p obtained from the NCNT.

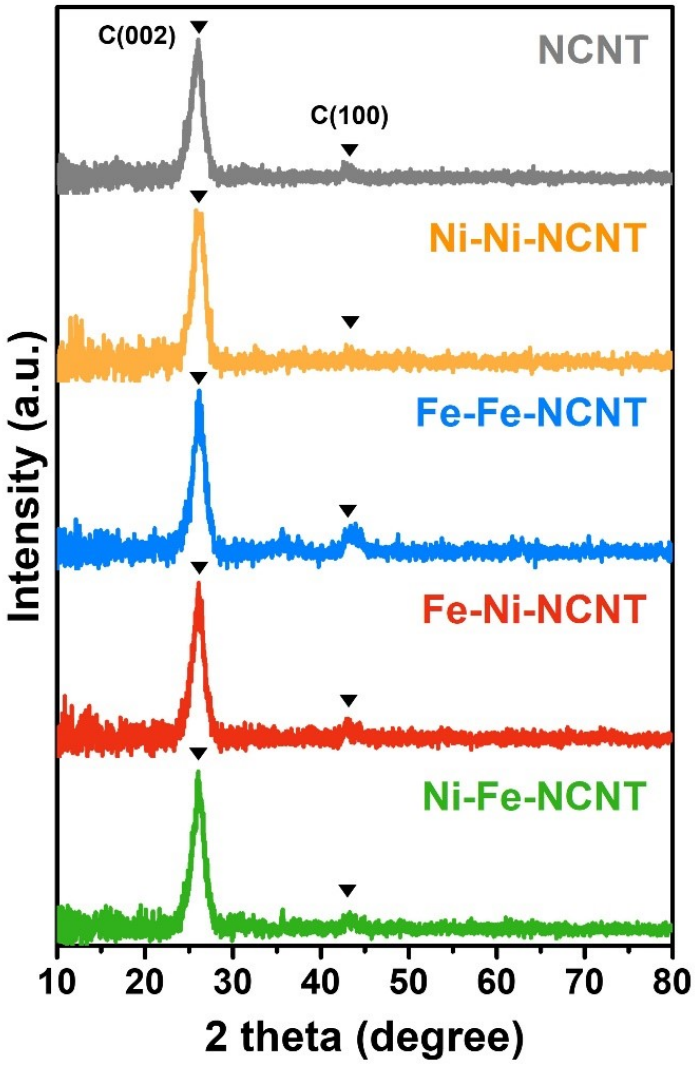

Figure S6. The X-ray diffraction (XRD) patterns obtained from the NCNT, Ni-Ni-NCNT, Fe-Fe-NCNT, Fe-Ni-NCNT and Ni-Fe-NCNT.

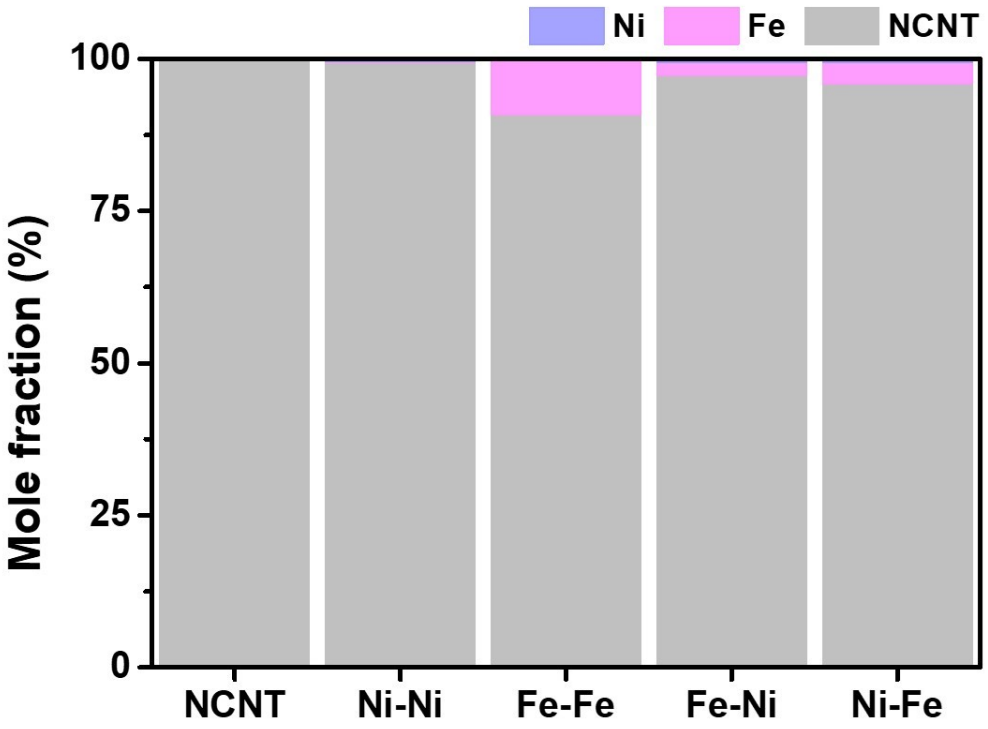

Figure S7. The mass spectrometry (MS) of NCNT, Ni-Ni-NCNT, Fe-Fe-NCNT, Fe-Ni-NCNT and Ni-Fe-NCNT.

	Ni-Ni-NCNT	Fe-Fe-NCNT	Fe-Ni-NCNT	Ni-Fe-NCNT
Metal fraction (%)	0.5	9.31	2.75	4.0

Table S1. The metal mole fraction of Fe-Fe-NCNT, Ni-Ni-NCNT, Fe-Ni-NCNT and Ni-Fe-NCNT.

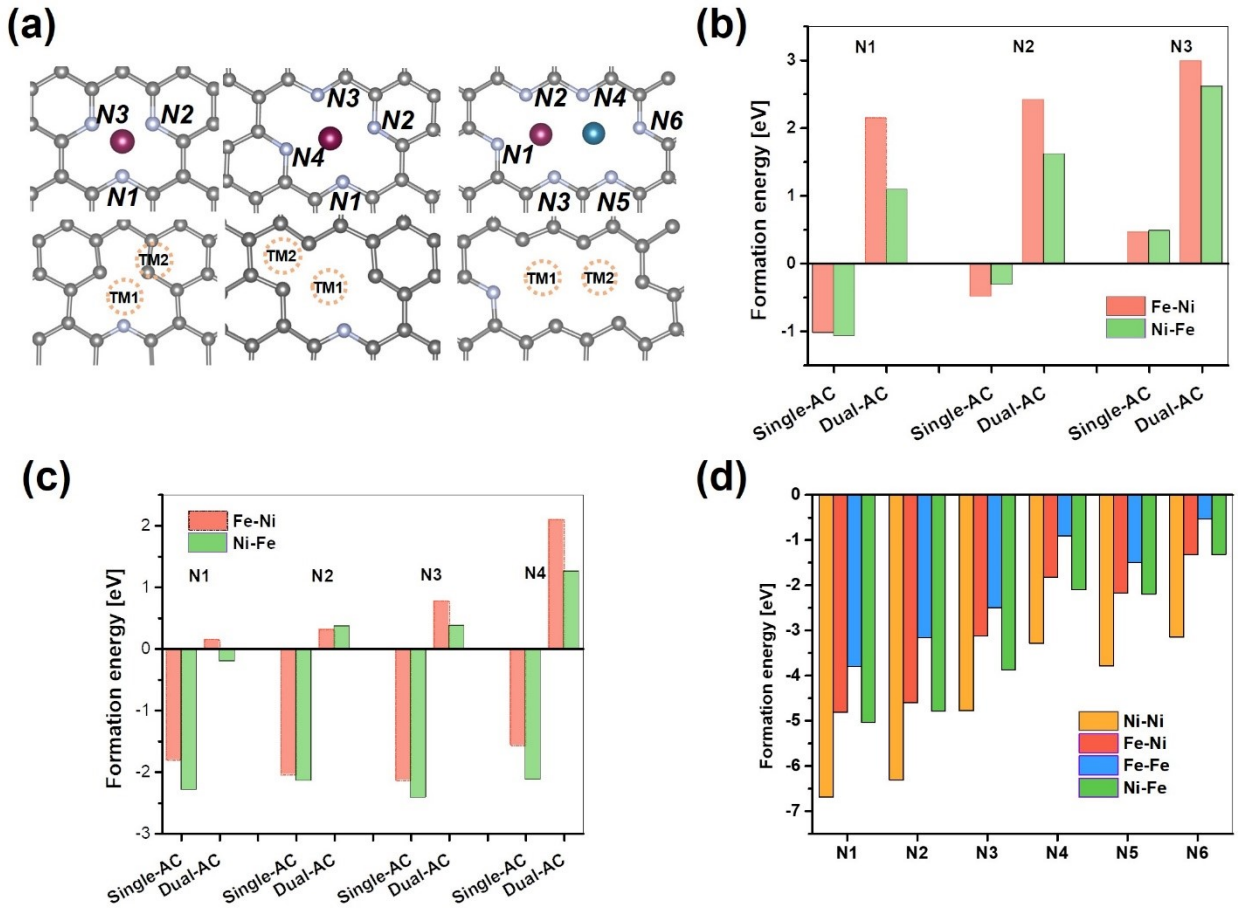

Figure S8. (a) Schematic of transition metal adsorption site and pyridinic structure. Transition metal adsorption sites were labeled as TM1 and TM2. Pyridinic structures were labeled as N1~N3 for single vacancy, N1~N4 for divacancy and N1~N6 for meso-pore vacancy structures. (b)-(d) Formation energy after adsorption of transition metal for single, di, and meso-pore vacancy. Single-AC and Dual-AC referred to single atom catalyst and dual atom catalyst. All substrates were named TM2-TM1 in the DFT calculation. The Single-AC denoted a configuration where only TM1 was adsorbed.

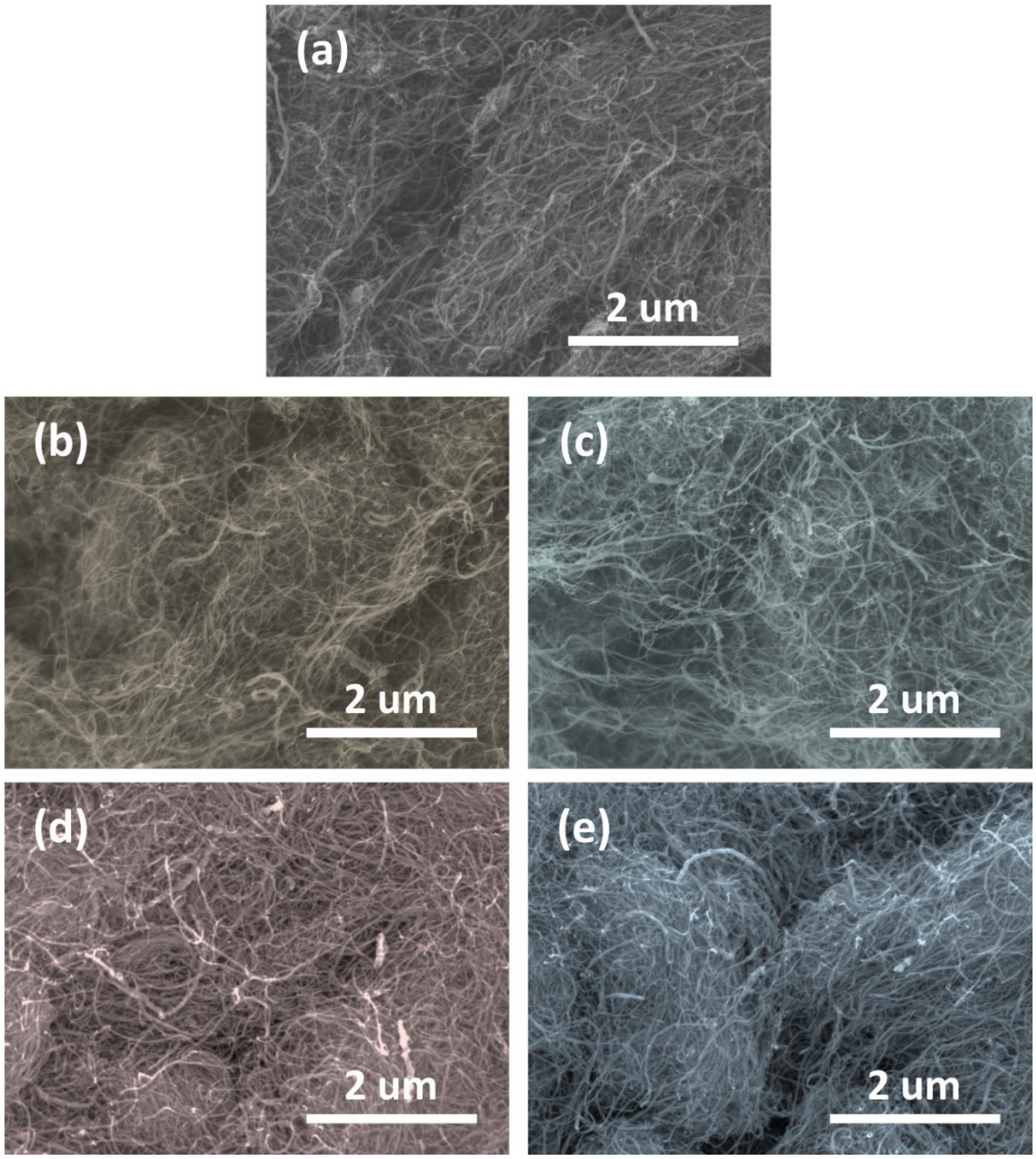

Figure S9. The scanning electron microscope (SEM) image obtained from (a) NCNT, (b) Fe-Fe-NCNT, (c) Ni-Ni-NCNT, (d) Fe-Ni-NCNT, (e) Ni-Fe-NCNT and (f) Ni/Fe-NCNT.

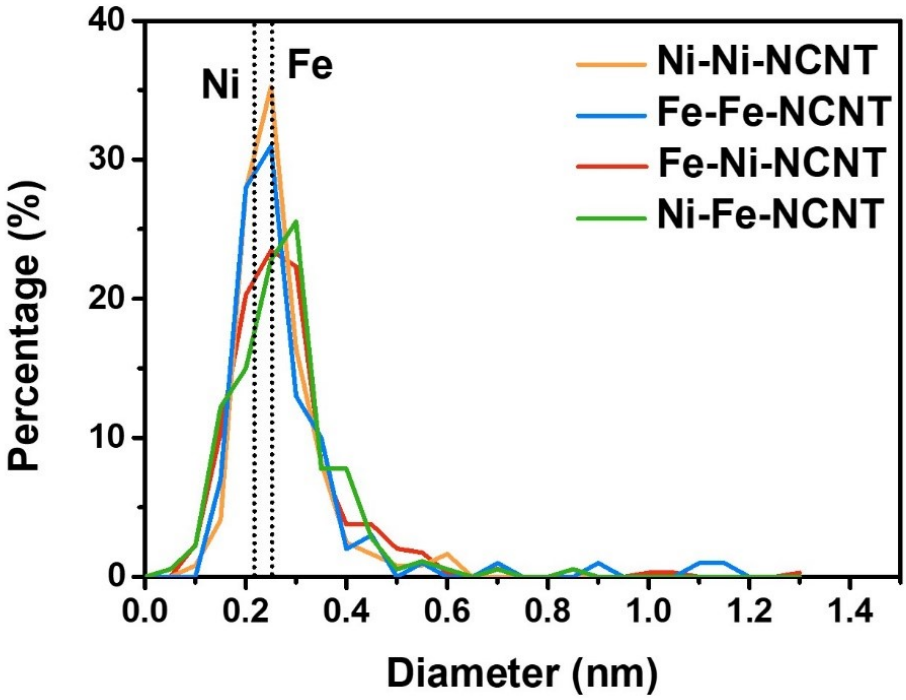

Figure S10. The metal particle size distribution of Ni-Ni-NCNT, Fe-Fe-NCNT, Fe-Ni-NCNT and Ni-Fe-NCNT.

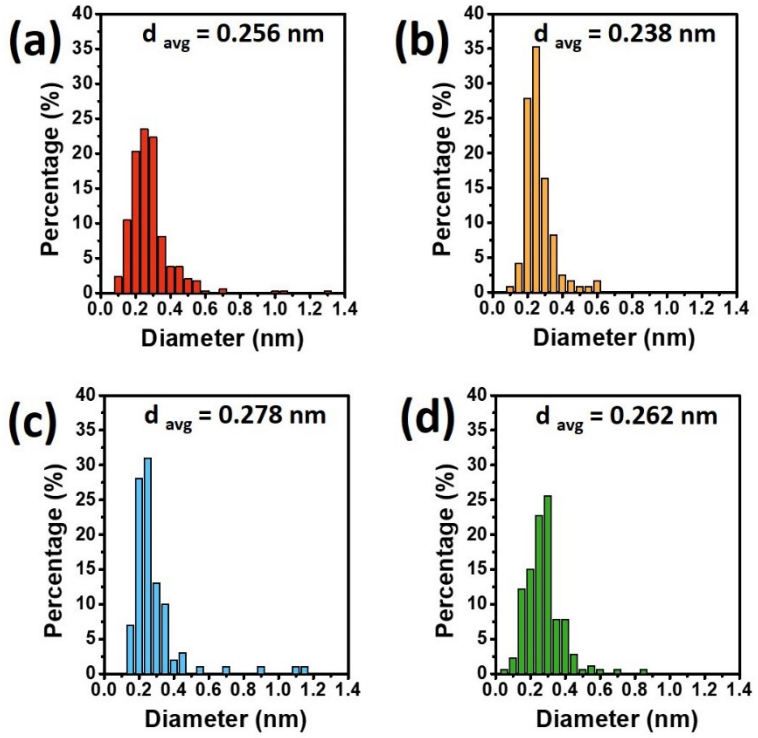

Figure S11. Metal particle size distribution of of (a)Fe-Ni-NCNT, (b)Ni-Ni-NCNT, (c)Fe-Fe-NCNT and (d)Ni-Fe-NCNT.

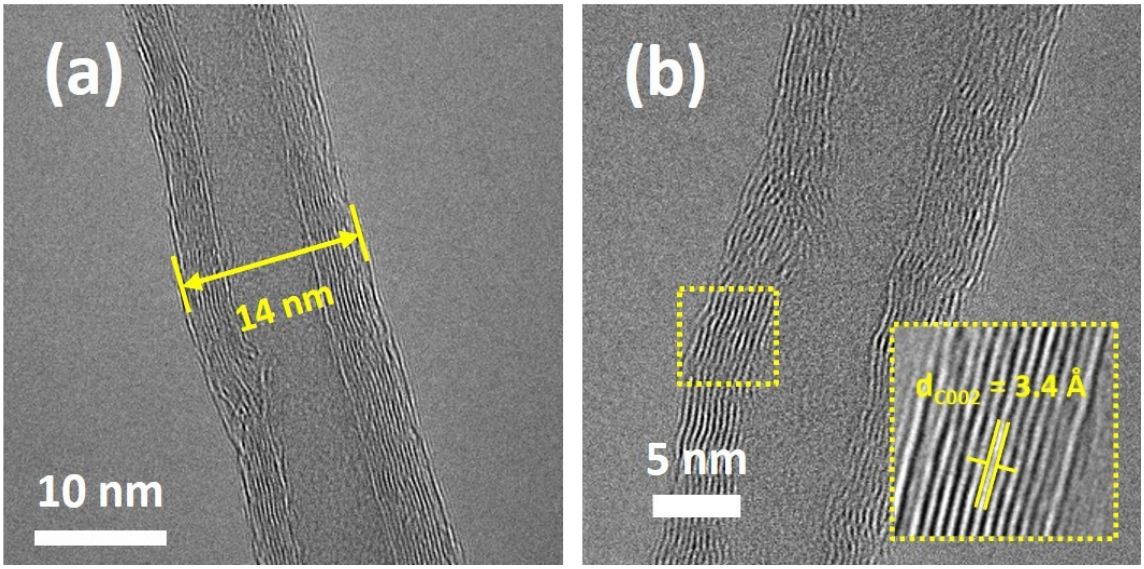

Figure S12. (a) The transmission electron microscopy (TEM) images and (b) the d-spacing analysis images of NCNT.

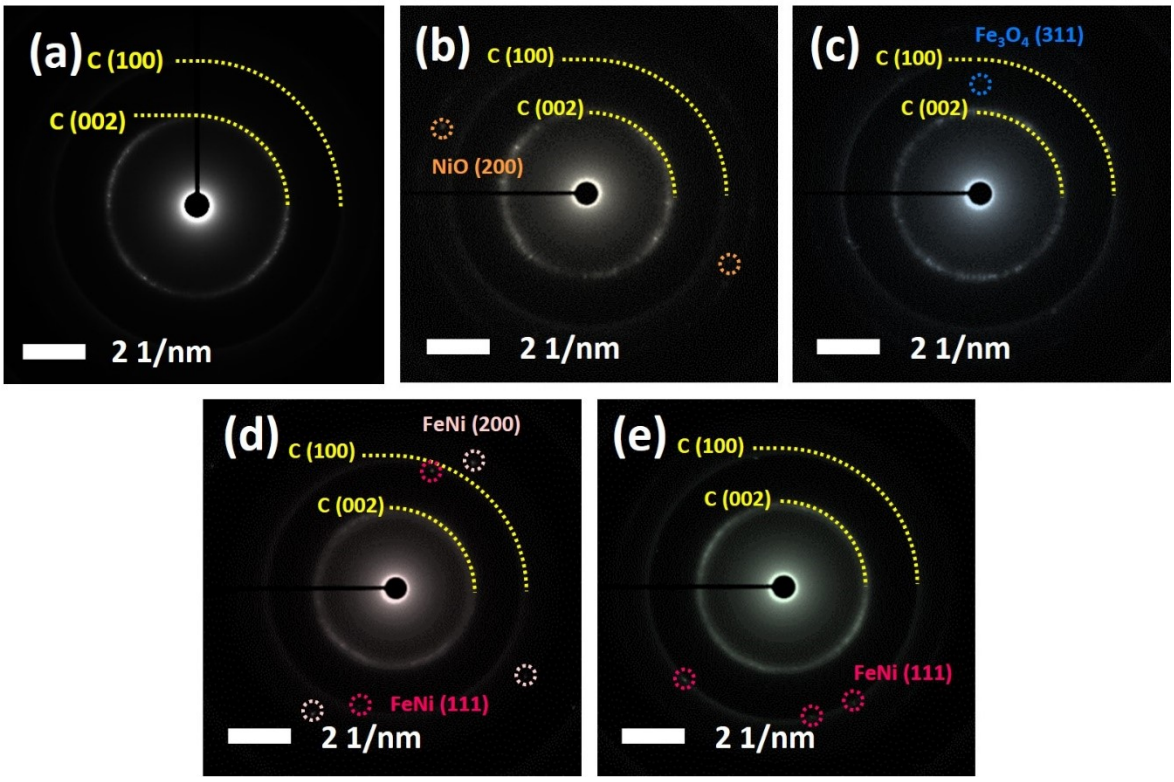

Figure S13. The selected area electron diffraction (SEAD) patterns image of (a) NCNT, (b) Ni-Ni-NCNT, (c) Fe-Fe-NCNT, (d) Fe-Ni-NCNT and (e) Ni-Fe-NCNT.

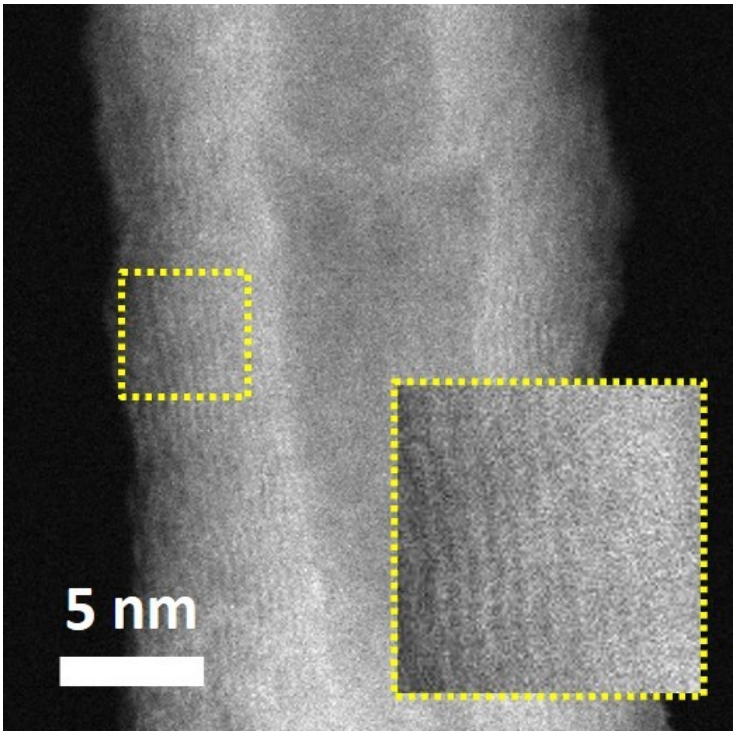

Figure S14. The scanning transmission electron microscopy (STEM) images of NCNT.

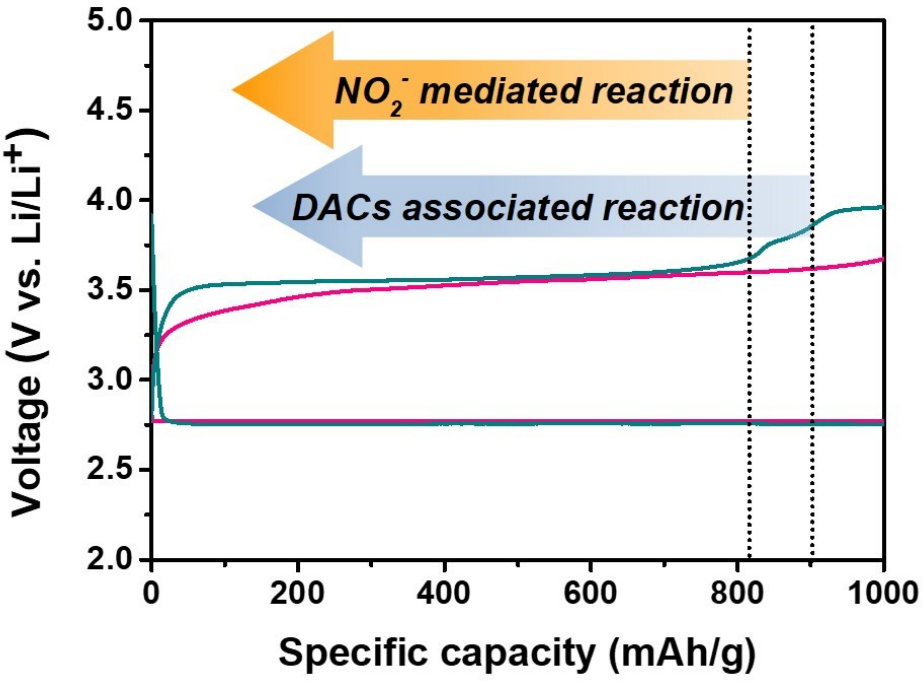

Figure S15. The OER mechanism analysis graph of Li-O_2 cell with DACs.

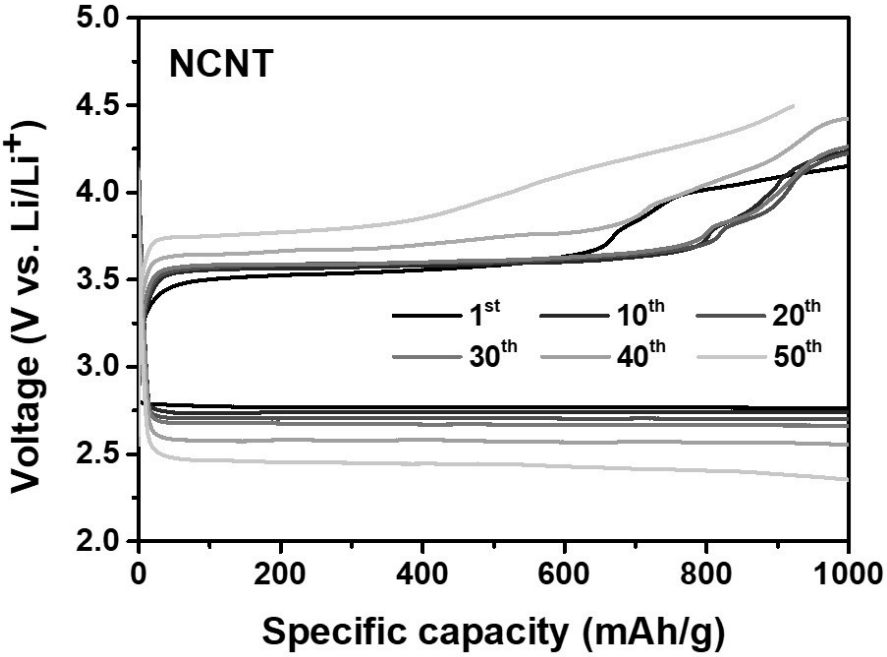

Figure S16. The cycle performance of NCNT in LOB cells.

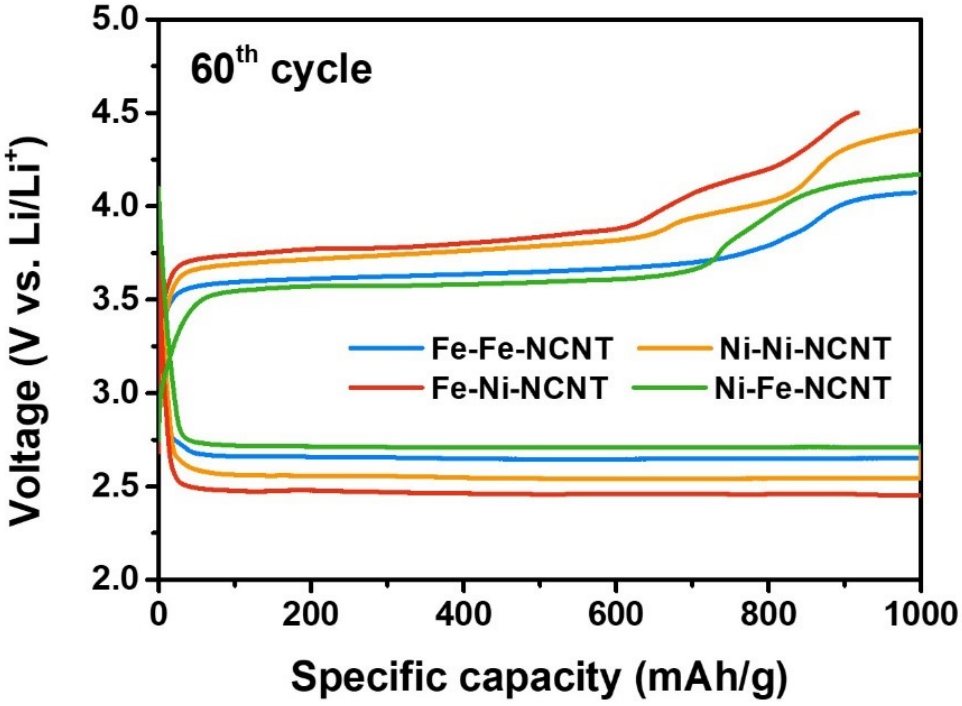

Figure S17. The 60th cycle performance of Fe-Fe-NCNT, Ni-Ni-NCNT, Fe-Ni-NCNT and Ni-Fe-NCNT.

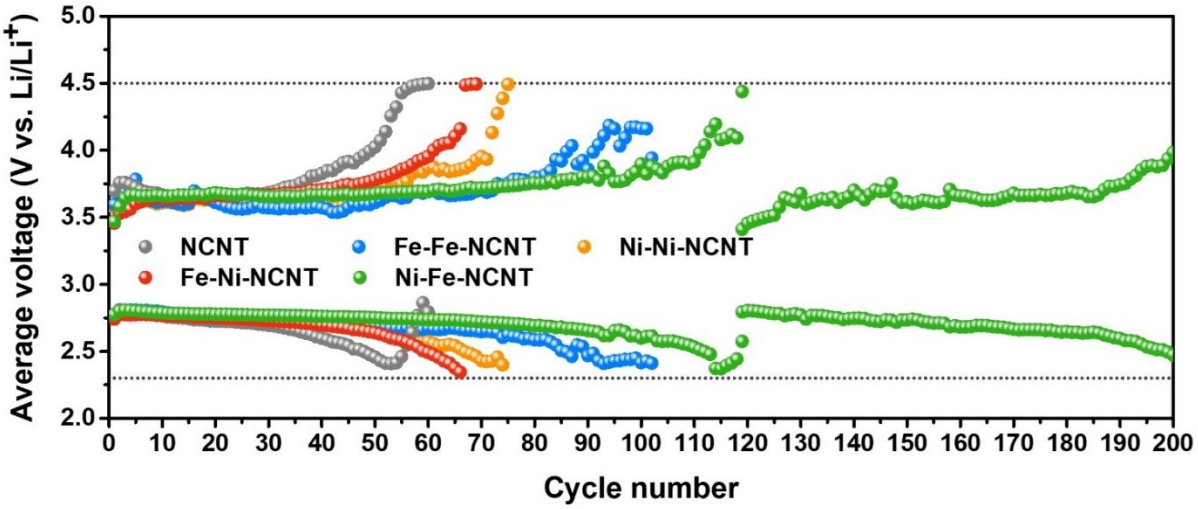

Figure S18. The average ORR and OER voltage of NCNT, Ni-Ni-NCNT, Fe-Fe-NCNT, Fe-Ni-NCNT and Ni-Fe-NCNT.

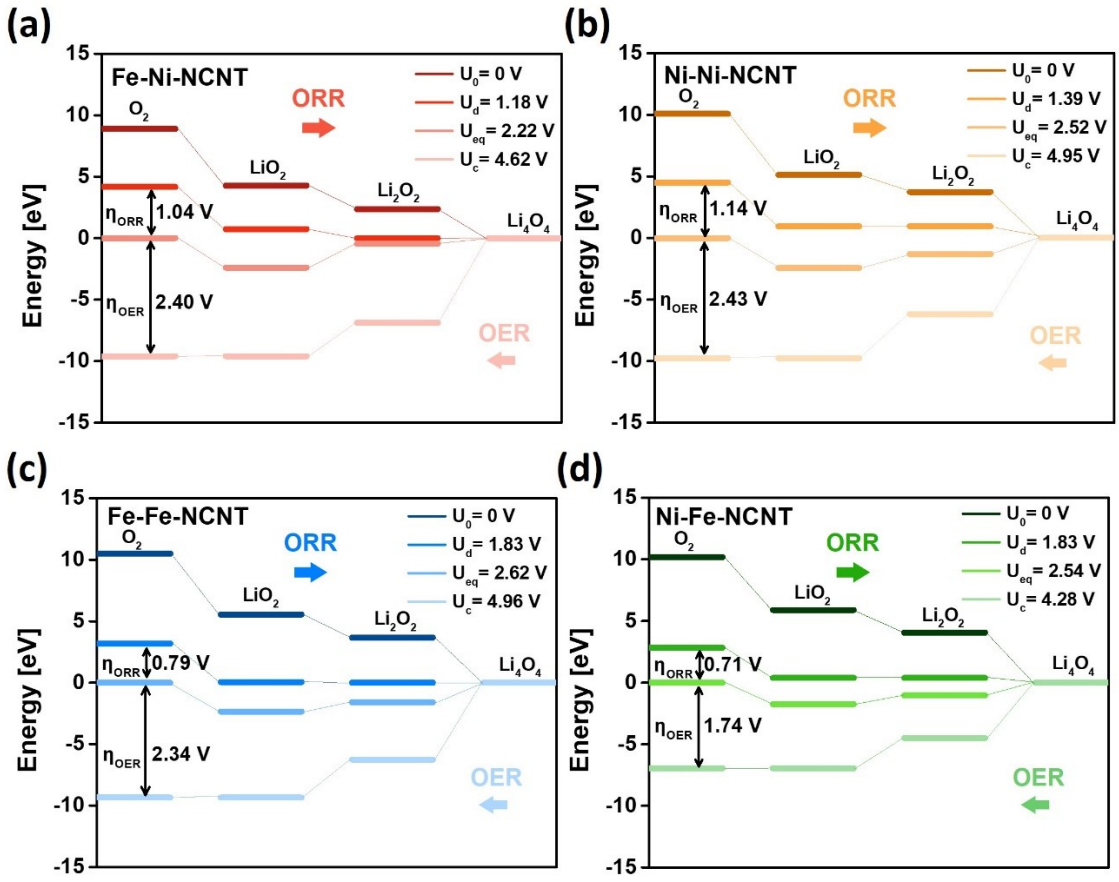

Figure S19 (a)-(d) Free energy diagram of OER/ORR in Ni-Ni-NCNT, Fe-Fe-NCNT, Fe-Ni-NCNT and Ni-Fe-NCNT.

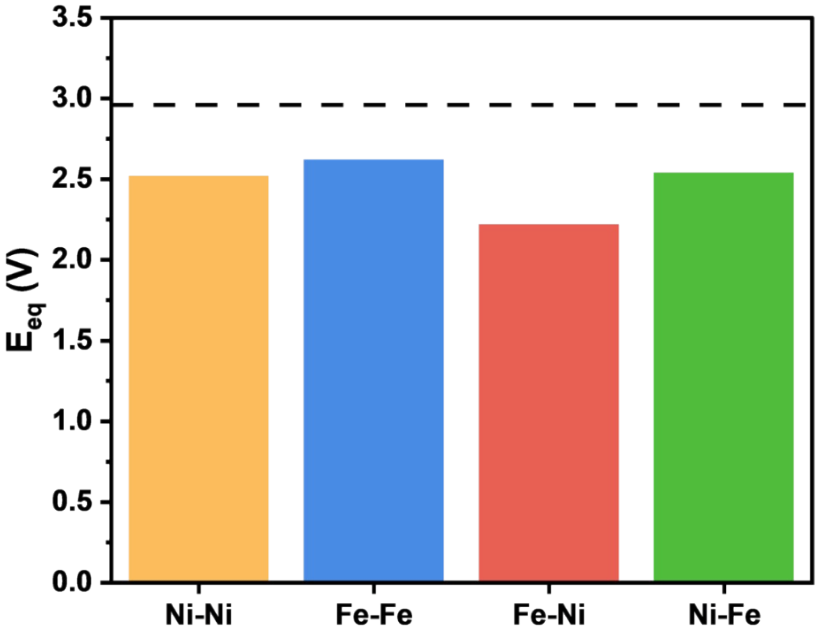

Figure S20 Equilibrium potential of all DACs cases. The dot line shows standard voltage, 2.96V.

Structure		Net charge (change)	
		Ni	**Ni**
Ni-Ni	Substrate	0.54	0.64
	LiO_2	0.81(+0.27e)	0.80(+0.16e)
	NO_2	0.90(+0.36e)	0.75(+0.11e)
		Fe	**Fe**
Fe-Fe	Substrate	0.91	1.01
	LiO_2	1.07(+0.16e)	1.21(+0.20e)
	NO_2	1.11(+0.20e)	1.23(+0.21e)
		Fe	**Ni**
Fe-Ni	Substrate	0.98	0.56
	LiO_2	1.15(+0.17e)	0.79(+0.23e)
	NO_2	1.35(+0.37e)	0.65(+0.09e)
		Ni	**Fe**
Ni-Fe	Substrate	0.42	1.33
	LiO_2	0.55(+0.13e)	1.78(+0.45e)
	NO_2	0.26(-0.16e)	2.26(+0.93e)

Table S2. Bader net charge and charge change value of transition metal after adsorption of LiO_2 & NO_2 on Ni-Ni-NCNT, Fe-Fe-NCNT, Fe-Ni-NCNT and Ni-Fe-NCNT.

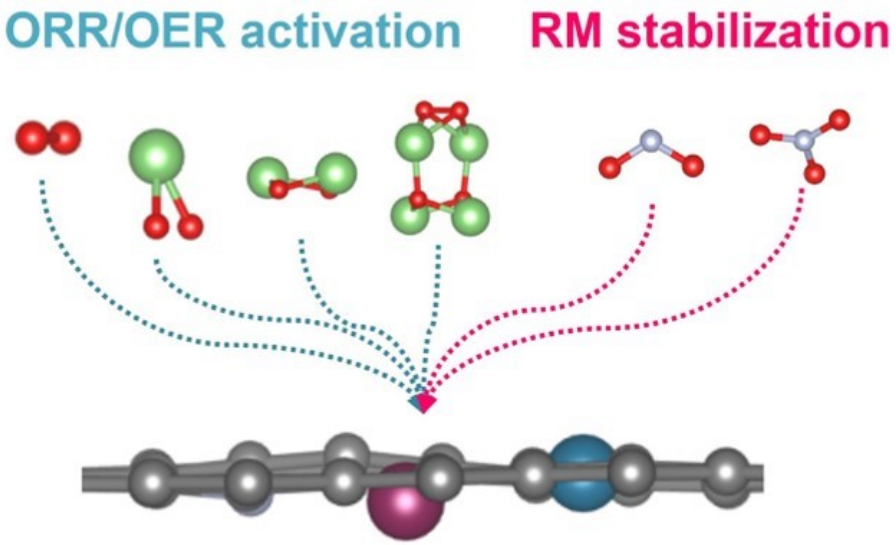

Figure S21. Schematic illustration for roles of DACs**.**

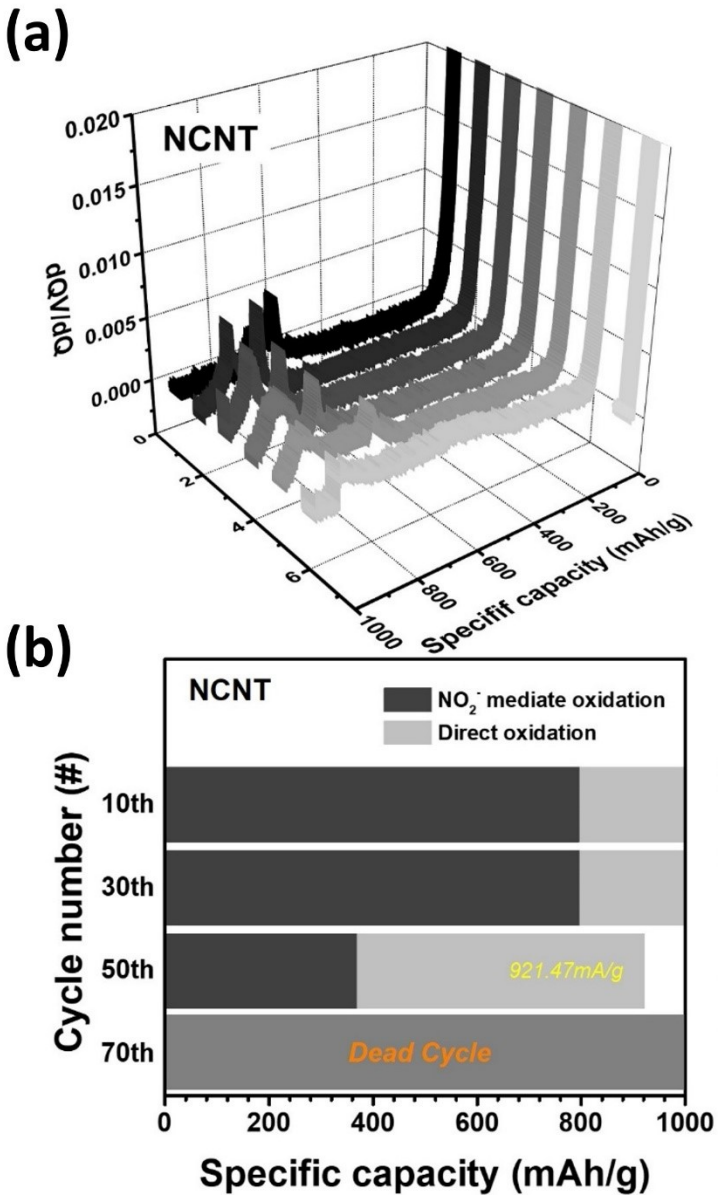

Figure S22. (a) The dV/dQ curves of the NCNT obtained from the 10th to the 70th cycle. (b) Ratios of "NO_2^- mediate oxidation", "DACs associated oxidation" and "Direct oxidation" of NCNT obtained from the 10th to the 70th cycle.

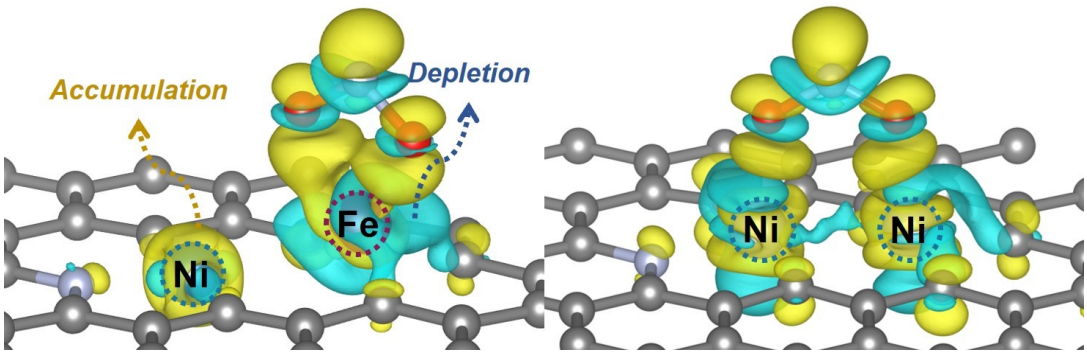

Figure S23. Calculated charge density difference plot NO_2 on Fe-Ni-NCNT and Ni-Ni-NCNT.